



Published in final edited form as:

Angew Chem Int Ed Engl. 2021 June 14; 60(25): 14163–14170. doi:10.1002/anie.202102453.

Discovery and biosynthesis of a structurally dynamic antibacterial diterpenoid

Chenxi Zhu^{†,‡,°}, Baofu Xu^{§,°}, Donovan A. Adpressa^{‡,°}, Jeffrey D. Rudolf^{†,§}, Sandra Loesgen^{*,†,‡,§}

[†]Department of Chemistry, Oregon State University, Corvallis, Oregon 97331, USA

[‡]Department of Analytical Research and Development, Merck & Co., Inc. Boston, MA 02115, USA

[‡]Whitney Laboratory for Marine Bioscience, University of Florida, St. Augustine, Florida 32080, USA

[§]Department of Chemistry, University of Florida, Gainesville, Florida, 32611, USA.

Abstract

A new bicyclic diterpenoid, benditerpenoic acid, was isolated from soil-dwelling *Streptomyces* sp. (CL12-4). We sequenced the bacterial genome, identified the responsible biosynthetic gene cluster, verified the function of the terpene synthase, and heterologously produced the core diterpene. Comparative bioinformatics indicated this *Streptomyces* strain is phylogenetically unique and possesses nine terpene synthases. The absolute configurations of the new *trans*-fused bicyclo[8.4.0]tetradecanes were achieved by extensive spectroscopic analyses, including Mosher's analysis, *J*-based coupling analysis, and computations based on sparse NMR-derived experimental restraints. Interestingly, benditerpenoic acid exists in two distinct ring-flipped bicyclic conformations with a rotational barrier of ~16 kcal mol⁻¹ in solution. The diterpenes exhibit moderate antibacterial activity against Gram-positive bacteria including methicillin and multi-drug resistant *Staphylococcus aureus*. This is the first isolation of an eunicellane-type diterpenoid from bacteria and the first identification of a diterpene synthase and biosynthetic gene cluster responsible for the construction of the eunicellane scaffold.

Graphical Abstract

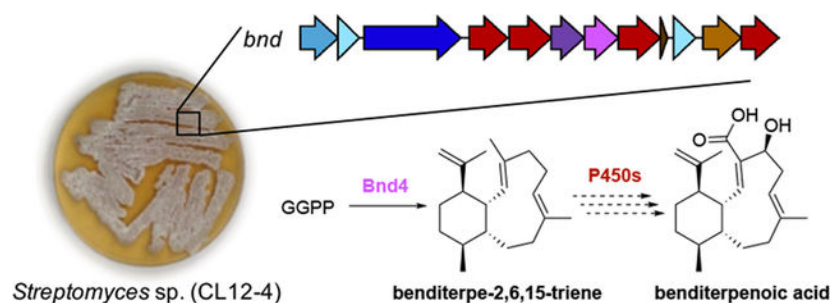
*Address for correspondence: jrudolf@chem.ufl.edu, sandra.loesgen@whitney.ufl.edu.

[°]Equal contributions

Publisher's Disclaimer: This manuscript has been accepted after peer review and appears as an Accepted Article online prior to editing, proofing, and formal publication of the final Version of Record (VoR). This work is currently citable by using the Digital Object Identifier (DOI) given below. The VoR will be published online in Early View as soon as possible and may be different to this Accepted Article as a result of editing. Readers should obtain the VoR from the journal website shown below when it is published to ensure accuracy of information. The authors are responsible for the content of this Accepted Article.

Conflicts of interest

The authors declare no conflict of interest.



We report the first isolation of an eunicellane-type diterpenoid from bacteria and the first identification of a diterpene synthase and biosynthetic gene cluster responsible for the construction of the eunicellane scaffold. The absolute configurations and antibacterial activities of benditerpenoic acid and the benditerpe-2,6,15-triene core were established.

Keywords

Natural Products; Diterpenoid; Terpene Synthase; Antibiotics; Absolute Configuration; DFT

Introduction

Terpenoids, found in all branches of the tree of life, are the largest and most structurally diverse class of natural products with more than 80,000 known compounds.^[1] Terpenoids exhibit a wide range of biological activities including, but not limited to, antibacterial, antifungal, antiparasitic, antiviral, anti-inflammatory, and immunomodulatory properties.^[2] Although these natural products were first, and are still most commonly, isolated from plants and fungi, bacteria are emerging as talented producers of unique and biologically active terpenoids.^[2b, 3] This fact coincides with the genomic knowledge supporting that bacteria possess an abundance of uncharacterized terpene synthases (TSs), the enzymes responsible for formation of the terpenoid core, and TS-encoding biosynthetic gene clusters (BGCs).^[4]

The first described terpenes from actinomycetes were the odoriferous geosmin and the camphor-like 2-methylisoborneol, both reported in the late 1960s and associated with the smell of wet soil.^[5] The advent of genome sequencing revealed that TSs are widely distributed in bacteria, particularly in actinomycetes, the workhorses of bacterial natural products.^[4, 6] In some cases (e.g., geosmin), the products of bacterial TSs are legitimate natural products and not simply biosynthetic intermediates on a pathway to more complex and functional terpenoids. Most terpenoid natural products, however, are highly functionalized scaffolds. Significant progress has been made in bacterial terpene chemistry by identifying unique TSs and characterizing their enzymatic products using heterologous expression or *in vitro* methods.^[4, 7] Yet, the biosynthetic products of TS-encoding BGCs continue to be exceedingly rare to find with one plausible reason being that many of these BGCs may be silent under laboratory conditions.^[4] Therefore, there is a clear need to bridge the gap between the products of TSs and their genuine natural products. Continued discovery of novel bacterial terpenoids and unique terpene scaffolds will facilitate future genome mining opportunities.

Herein, we report the isolation and characterization of a newly discovered diterpenoid scaffold produced by a *Streptomyces* sp., isolated from arid, high desert soil near Bend, Oregon. Due to the slow chemical exchange from two ring-flipped conformers for benditerpenoic acid (**1**) and four conformers for the unfunctionalized core benditerpe-2,6,15-triene (**2**) in solution, structure elucidation by NMR spectroscopy was a significant challenge. The natural occurring *trans*-fused bicyclo[8.4.0]tetradecane contains five stereogenic centers, the heterologously expressed core exhibits four stereocenters, and both exhibit two double bond geometries within the bicycle. The absolute configurations of the new diterpenoids were assigned independently as 1*S*, 2*Z*, 4*S*, 6*E*, 10*R*, 11*S*, 14*R* for benditerpenoic acid and 1*S*, 2*E*, 6*E*, 10*R*, 11*S*, 14*R* for the benditerpe-2,6,15-triene core using a combination of Mosher ester analysis^[8], 2D NMR experiments including *J*-based analysis (JBCA)^[9], and computational modeling. Subsequent genome sequencing and bioinformatic analysis revealed the BGC responsible for the production of **1**. Finally, biochemical characterization of benditerpe-2,6,15-triene synthase, the type I TS encoded within the *bnd* BGC, confirmed it constructs the *trans*-fused bicyclo[8.4.0]tetradecane scaffold from GGPP and provided insight into the biosynthesis of **1**.

Results and Discussion

Isolation and structural elucidation of benditerpenoic acid

Bioactivity-guided fractionation (Figure S1) led to the isolation of benditerpenoic acid (**1**) as a white powder with a chemical formula of C₂₀H₃₀O₃ based on HRESIMS *m/z* 319.2269 (δ ppm = 0.3; calcd for C₂₀H₃₁O₃⁺ 319.2268; Figure S2). The UV spectrum exhibited absorbance maxima at 210 and 228 nm (Figure S3) and its IR bands were supportive of hydroxyl groups (3446 cm⁻¹) and carbonyl (1697 cm⁻¹), and a terminal alkene (2922 cm⁻¹). The structure and relative configuration of the new terpenoid was derived from ¹H-, ¹³C- and 2D NMR experiments, including COSY, NOESY, ROESY, TOCSY, HSQC and HMBC (Table S1, Figure 1A and 1B, Figures S4–S20); detailed analysis of the NMR data resulting in the structural elucidation of **1** can be found in the Supporting Information. Observation of doubled resonances from both proton and carbon spectra as well as chemical exchange crosspeaks in NOESY spectra suggested that **1** undergoes slow chemical exchange.

To determine the relative and absolute configuration of benditerpenoic acid (**1**), which possesses five asymmetric carbon centers and a flexible, bicyclic ring system, modified Mosher ester analysis,^[8] analysis of NOESY and *J*-based couplings supported by density functional theory (DFT) computations were used.^[9] Mosher ester analysis unequivocally determined C-4 to be *S* configured (Figure 1C, Figure S21). With the absolute configuration of the secondary alcohol defined, NOESY and *J*-based conformational analysis were used to determine the remaining four stereocenters. H-1 exhibits a doublet of doublets of doublets (ddd) pattern with two large coupling constants (11.0 and 10.3 Hz) and one small one (4.3 Hz), indicating two *trans* and one *cis* relationship between this and the adjacent stereocenters of the decalin ring system. Based on the DQF-COSY data extraction, the ³*J*_(H-2,H-1) coupling constant is 10.0 Hz in both conformers supporting the orientation to be *trans* and accounting for one of the two large coupling constants within the ddd multiplet of H-1 (Figure S16–18). The NOESY spectrum showed a strong NOE correlation from H-1 to CH₃-17, placing

them *cis* to one another and accounting for the second large coupling constant ($^3J_{\text{H-1,H-14}} = 11.0$ Hz). This was further corroborated by a very weak NOE correlation from H-1 to H-14 suggesting a *trans* orientation (Figure S9). Thus, H-1 and H-10, supported by the small coupling constant ($^3J_{\text{H-1,H-10}} = 4.3$ Hz) have a *cis* configuration. Additionally, a strong NOE between H-1 and H-18 indicates a *cis* configuration. A strong NOE correlation between H-2 and H-4 was found in both conformers in the NOESY spectrum, setting the geometry of the C-2/C-3 double bond as *Z*. IPAP-HMBC NMR data displayed the $^3J_{\text{(H-6,C-19)}}$ coupling to be approximately 7 Hz in both ring conformers indicating that the C-6/C-7 double bond is *E* configured (Figure S19).^[10] A very small coupling constant $^4J_{\text{(H-1,C-18)}}$, approximately 1 Hz, suggests a *cis* configuration between H-1 to C-18 (Figure S20). These values were corroborated by DFT calculations of coupling constants (see SI for more detail). Combined, the Mosher ester analysis, NOESY data, and JBCA provide an absolute configuration of 1*S*,2*Z*,4*S*,6*E*,10*R*,11*S*,14*R* for **1**. Next, we employed 3D structural computation of conformers to support the assignment of the absolute configuration. Here, the conformational space of **1** was calculated using ForceGen (BioPharmics LLC, v4.4) by applying minimal distance and torsion restraints derived from NOE and *J* values, namely the observed NOE between H-1 and H-4 and between H-1 and 18-CH₃, and the $^3J_{\text{HH}}$ between H-1 and H-2, to guide accurate conformational sampling (Figure 2A).^[11] From this conformational ensemble, the Boltzmann population was computed by DFT at the MPW1PW91/cc-PVTZ level and the two lowest energy conformers were found to exhibit an up/down flip of the bicyclic ring (Figure 2C). The bicycle has two distinct low energy forms (i.e., methyl up in green and methyl down in purple) with nearly identical energies. Metadynamics simulations indicated a rotational barrier from a low energy conformation, through a local minimum, to the other low energy minimum, with an ~16 kcal mol⁻¹ maximum barrier pathway between the two minima (Figure 2D). This observation explains the chemical exchange shown in the NOESY/ROESY spectra of **1**. The Boltzmann populations are approximately 3:2, which matches the integration ratios observed in the ¹H NMR (Table S1). Computationally derived UV and ECD data at the ωB97XD/def2TZVP//MPW1PW91/cc-PVTZ level compared with experimental spectra further support the stereochemical assignment of benditerpenoic acid (**1**) (Figure S22).

Structurally related compounds

Compared with other families of diterpenoids, bacterial diterpenoids are rare.^[2b] The closest structural relatives are the 6,8,4- and 6,7,5-tricyclic odyverdienes and 6,10-bicyclic pre-hydrophyrene, which were isolated from the heterologous expression of di-TSs (i.e., not as genuine natural products; Figure S23).^[7b, 12] Interestingly, pre-hydrophyrene is reported as a neutral, but unstable, intermediate on the pathway to hydrophyrene and hydrophyrenol, which feature unique 6,6,6,6-tetracyclic scaffolds.^[7b, 12] The 6,10-bicyclic eunicellane scaffold has been found in corals^[13] with examples including the solenopodins,^[14] klysimplexins,^[15] and excavatolides (Figure S23).^[16] Some references allude to their dynamic behavior in solution and the challenges encountered when assigning their respective structures.^[16b] Recently, vibrational circular dichroism experiments and computational approaches were used to elucidate the absolute configuration of Gorgonian-derived briaranes.^[17] Of these structurally related diterpenoids, there are no known bacterial natural products with the eunicellane-type skeleton nor known di-TSs responsible for constructing the 6,10-bicyclic

eunicellane core. Although the 6,10-bicyclic skeletons of **1** and the coral eunicellanes are the same, the differences in their stereocenters and double bond placement and configurations suggest that the di-TSs that construct these 6,10-bicyclic skeletons are different.

Identification of the *bnd* BGC by genome mining for unique TSs

Given the novelty of the eunicellane-type skeleton of **1** from bacteria, we sought to identify the TS and BGC responsible for constructing and functionalizing the 6,10-bicyclic core. We sequenced the genome of *Streptomyces* sp. (CL12-4) using Oxford Nanopore and Illumina sequencing technologies. The draft genome is ~9.01 Mb in total length, 71.92% GC content, and currently assembled into 16 contigs with the largest contig ~2.05 Mb; two contigs were assembled into circular plasmids of 0.13 and 0.08 Mb. A multi-gene phylogenetic analysis of *Streptomyces* sp. (CL12-4) positioned it in its own clade near *Streptomyces ambofaciens* (five-gene concatenation 97.6% sequence identity) and *Streptomyces rochei* (96.8%) (Figure S24).

Using a combination of antiSMASH^[18] and BLAST^[19], we detected a total of nine putative TSs encoded within the genome. Sequence comparisons and phylogenetic analysis of these nine TSs with characterized TSs from *Streptomyces* revealed two sesqui-TSs (germacradienol/geosmin and (+)-*epi*-isozizaene synthases), one putative di-TS, and six additional proteins that are highly similar to ubiquitous TSs such as phytoene synthase (Figure 3A). The candidate di-TS, later named Bnd4, claded with the di-TS SCLAV_p1169, a clavulatriene synthase from *Streptomyces clavuligerus*,^[4, 7b] with pairwise alignment between Bnd4 and SCLAV_p1169 showing only 29% sequence identity. As phylogenetic clading of bacterial TSs can be misleading due to high sequence disparities between TSs, we next constructed a sequence similarity network (SSN) of all known and putative TSs from the Streptomycetaceae family (Figure 3B).^[20] At an e-value threshold of 10^{-60} , many families of TSs segregate into individual subfamily clusters. Bnd4 was found in an uncharacterized subcluster with eight other TSs. SCLAV_p1169, odyverdiene synthase, and hydropyrene synthase were all found as singletons, highlighting their diverse sequences.

Sequence analysis of Bnd4 and eight highly homologous (>40% identity) TSs revealed canonical DDxxD and NSE metal-binding motifs as well as the C-terminal WxxxxxRY motif that is responsible for guiding product formation (W) and sensing the diphosphate moiety (RY) (Figure S25).^[21] The NSE and WxxxxxRY motifs are strictly conserved in these TSs, but four Bnd4 homologues do not have a complete DDxxD motif (e.g., *Amycolatopsis arida* has a DDxxV motif; *Amycolatopsis taiwanensis* has a GNNA motif).

Characterization of a novel diterpene synthase and structural elucidation of the core diterpene scaffold

To confirm whether Bnd4 and the BGC that encodes it is responsible for the biosynthesis of benditerpenoic acid (**1**), we cloned *bnd4* into *E. coli* and produced and purified Bnd4 for in vitro biochemical characterization (Figure S26). Incubation of Bnd4 with geranylgeranyl diphosphate (GGPP) resulted in the formation of a single non-polar product named benditerpe-2,6,15-triene (**2**) (Figure 4A). We also individually incubated Bnd4 with geranyl

diphosphate (GPP) and farnesyl diphosphate (FPP) but only saw minor amounts of geraniol, farnesol, and a few additional unknown products (Figure S27).

Inspired by previously successful diterpene production in *E. coli*,^[22] we constructed a three-plasmid system for diterpene production. We subcloned *bnd4* into pET21a yielding pJR1017 and transformed *E. coli* BL21 Star (DE3) harboring pJR1015 and pJBEI-2999,^[23] which encode a GGPP synthase and an FPP overproduction system, respectively, with pJR1017. We also created a two-plasmid system harboring only pJR1017 and pJR1015 to test whether pJBEI-2999 enhanced the yield of benditerpe-2,6,15-triene (**2**). While both constructs produced **2**, the three-plasmid system had a significantly higher titer (Figure S28).

A large scale (12 L) culture of the three-plasmid system in *E. coli* resulted in the isolation of 10.7 mg of **2**. GC-MS analysis of **2** afforded an M⁺ peak with an *m/z* of 272, consistent with that of a diterpene skeleton, but the MS spectrum was unique when compared with the NIST reference database (Figure 4B, Figure S29). NMR elucidation was based on 1D and 2D NMR experiments (Figures S30–S35). Full assignment was achieved using CDCl₃ as solvent at room temperature (Table S1) and supported by higher temperature experiments at 70 °C in C₆D₆, which reduced peak broadening due to conformational flexibility (Figure S36). Briefly, the planar structure was established by spin systems found in the six- and ten-membered rings via COSY and HMBC correlations (Figure 4C). Similar to **1**, key NOESY correlations were found between CH₃-18 and H-10 and CH₃-18 and H-1, placing them both syn in regard to the bicyclic system; H-1 and H-10 also showed a NOESY crosspeak. No correlation between H-14 and H-1 was interpreted as anti configuration. Analogous to **1**, NMR and DFT-based computations were used to assign the relative and absolute configuration of **2**. JBCA and subsequent modeling of the proposed multiplet (ddd, *J* = 12.4, 9.0, 4.2 Hz) indicates **2** has the same 1*S**,10*R**,14*R** relative configuration as **1**. NOE correlations from H-1 to CH₃-17 and CH₃-18 indicate these groups are *cis* to H-1. The double bond geometry was derived from *J*-based analysis using IPAP-HMBC NMR experiments which yielded ³*J*_(H-2,C-20) and ³*J*_(CH₃-20,C-2) coupling constants of 8.9 Hz (calculated 8.0 Hz) and 5.6 Hz (calculated for 4.8 Hz), respectively, supporting assignment of the C-2/C-3 double as *E* configured (Figure S37). C-6/C-7 was also assigned as *E* configured based on the ³*J*_(H-6,C-19) and ²*J*_(H-6,C-5) coupling constants of 6.4 Hz (calculated 4.5 Hz) and 4.9 Hz (calculated for 4.9 Hz), respectively. Considering the biosynthetic logic and the relative configuration of **2** is identical to that of **1**, we concluded that the absolute configuration of **2** is 1*S*,2*E*,6*E*,10*R*,11*S*,14*R*. In solution, four conformers account for 98.7% of the conformational space of **2** (Figure S38). Recently, a 6,10-bicyclic intermediate with the same absolute configuration of **2** was proposed in the cyclization mechanism of catenul-14-en-6-ol synthase (CaCS), using comprehensive isotopic labeling experiments, benditerpetriene, however, is not formed by CaCS.^[24] Bnd4 and CaCS only share 23% sequence identity with 52% coverage. These data, taken together, support the functional assignment of Bnd4 as a product-specific benditerpe-2,6,15-triene synthase.

Proposed biosynthesis of benditerpenoic acid (**1**) via benditerpe-2,6,15-triene (**2**)

After confirming that Bnd4 generates the same 6,10-bicyclic scaffold seen in **1**, we next analyzed the genetic neighborhood of *bnd4* to identify the BGC responsible for

the biosynthesis of **1**. *bnd4* is located within a promising BGC that encodes a GGPP synthase (*bnd3*), three cytochromes P450 (*bnd1*, *bnd2*, and *bnd5*), a ferredoxin (*bnd6*), and a complement of regulatory proteins and a transporter (Figure 4D). In fact, *bnd1–bnd6* are predicted to be encoded within a single operon. A fourth P450 (*orf3*) and an acyltransferase (*orf2*) are found downstream of the *bnd* cluster; however, it is unclear whether these are involved in the biosynthesis of **1**. There are only two oxidative transformations, a six-electron oxidation of CH₃-20 and a stereoselective hydroxylation at C-4, required to process **2** into **1**. Therefore, we propose that after Bnd4 forms **2** from GGPP, which is synthesized by Bnd3, the 6,10-bicyclic carbon skeleton is sequentially oxidized by the encoded P450s. It is tempting to speculate why these neighboring genes are present, based on the fact that only one natural product was detected and isolated in our culture conditions. For example, three or four P450s are present but unlikely to be required for the two oxidative transformations, particularly given that a single P450 is capable of catalyzing the six-electron oxidation of a methyl group into a carboxylic acid.^[25] Sequence analysis of the four P450s revealed that each P450 possesses the axial Cys and other commonly conserved motifs and residues found in functional P450s from *Streptomyces*.^[26] Overall, the genes might be involved in the extended biosynthesis of a more complex natural product which we did not detect or may confer resistance to **1**. Future studies are planned to elucidate the roles, if any, of these genes in the biosynthesis of **1**.

In order to evaluate whether the eight highly homologous TSs of Bnd4 are predicted to biosynthesize **1**, we first annotated their genetic neighborhoods and aligned the BGCs with Clinker (Figure 5).^[27] In fact, each of the BGCs encodes the core biosynthetic genes with each of the BGCs from *Streptomyces* identical in genetic organization, with the exception of the lack of the transporter in *Streptomyces* sp. CNH287 and *Streptomyces* sp. yr375. While the BGC from *A. arida* possesses the five core genes, the organization is different, includes an isoprenoid precursor gene and the downstream acyltransferase (*orf2* in CL12-4) and additional P450 (*orf3* in CL12-4), suggesting they may in fact be biosynthetically related, perhaps in the biosynthesis of a natural derivative of **1**. Two additional BGCs from *A. taiwanensis* and *Nocardia* sp. SYP-A9097 encode similar cohorts of genes as well as type I polyketide synthases (Figure 5). Having access to *A. arida*, we sought to determine whether its homologous TS (71.6% identity to Bnd4), TS^{Aa}, produces **2**. As with Bnd4, we heterologously produced TS^{Aa} in *E. coli* and confirmed that it converts GGPP into **2** in vitro (Figure 4A and S26). Therefore, while its BGC is different to that in *Streptomyces* sp. (CL12-4), the terpene core is identical. This may support that the 6,10-bicyclic scaffold of **2** is used to biosynthesize additional unique natural products in bacteria.

Activity

Both new terpenoids were screened for cytotoxicity in mammalian cancer cells^[28] and antimicrobial activity in a panel of Gram-positive and Gram-negative bacteria and the pathogenic yeast *Candida albicans*.^[29] Against Gram-positive bacteria, **1** exhibits moderate activity against the spore-forming bacterium *Bacillus subtilis*, a laboratory surrogate for *Bacillus anthracis*, and the human pathogen *Enterococcus faecium* with MIC values of 32 and 128 $\mu\text{g mL}^{-1}$. Moderate anti-staphylococcal activity was observed against *S. aureus*, methicillin-resistant *S. aureus*, and multi-drug resistant *S. aureus* with MIC values of 64,

64, and 128 $\mu\text{g mL}^{-1}$, respectively. The unoxidized benditerpe-2,6,15-triene (**2**) is less active than **1** (Table 1). No cytotoxicity was observed in single dose assays for **1** or **2** against five mammalian cell lines (at 10 μM), *C. albicans*, and the tested Gram-negative bacteria (at 100 μM).

Conclusion

In summary, we discovered the first bacterial eunicellane-type diterpenoid antibiotic from a soil-dwelling *Streptomyces* sp. (CL12-4). Using genome sequencing and genome mining, we identified the responsible BGC and characterized the unique TS that generates the *trans*-fused bicyclo[8.4.0]tetradecane scaffold of benditerpenoic acid. Both, the natural product and heterologously expressed benditerpe-2,6,15-triene core, are structurally complex with five and four stereocenters, respectively, and two double bond geometries in a fused bicyclo[8.4.0]tetradecane scaffold. Extensive spectroscopic analyses, including Mosher's analysis, *J*-based coupling analysis, and computations based on sparse NMR-derived experimental restraints, independently established the absolute configurations. It is noteworthy that these novel diterpenoids are dynamic, existing in distinct ring-flipped conformers in solution, and begs the question if this ring flexibility impacts its downstream biosynthetic steps and therefore can modulate the biological activity. Benditerpenoic acid was moderately active against a panel of Gram-positive bacteria while the benditerpe-2,6,15-triene core was less active. This study, and the prevailing literature,^[2b] supports that bacteria are a reservoir for novel terpene scaffolds, terpenoid natural products, and terpene synthases.

Supplementary Material

Refer to Web version on PubMed Central for supplementary material.

Acknowledgements

This work was supported by OSU (SL) and UF start-up funds (SL and JDR) and by NIH Grant R00 GM124461 (JDR) and NSF Grant 1808717 (SL). We wish to thank Elizabeth N. Kaweesa, Dr. Birte Plitzko for assisting with cell viability assays, Paige E. Mandelare for antifungal assays, Cassandra Lew for support in culture processing, and Eugene Kwan in metadynamics calculations. We wish to thank Steve Huhn (OSU) and James Rocca (UF) for excellent NMR support and Jodie Johnson for GC-MS support. We acknowledge the support of the Oregon State University's NMR Facility funded in part by the National Institutes of Health, HEI Grant 1S10OD018518, and by the M. J. Murdock Charitable Trust grant #2014162. We acknowledge the University of Florida's McKnight Brain Institute at the National High Magnetic Field Laboratory's Advanced Magnetic Resonance Imaging and Spectroscopy (AMRIS) Facility, which is supported by the US NSF Cooperative Agreement No. DMR-1644779 and the State of Florida. Some NMR spectra were acquired using a unique 1.5 mm High Temperature Superconducting Cryogenic Probe developed with support from the NIH (R01 EB009772). We also thank the University of Florida's Mass Spectrometry Research and Education Center (MSREC), which is supported by the NIH S10 OD021758-01A1.

References

- [1]. a) Dickschat JS, Nat. Prod. Rep 2016, 33, 87–110; [PubMed: 26563452] b) Lange BM, Annu. Rev. Plant Biol 2015, 66, 139–159. [PubMed: 25621517]
- [2]. a) Huang M, Lu J-J, Huang M-Q, Bao J-L, Chen X-P, Wang Y-T, Exp. Opin. Investig. Drugs 2012, 21, 1801–1818; b) Rudolf JD, Alsup TA, Xu B, Li Z, Nat. Prod. Rep 2021, DOI 10.1039/D0NP00066C; c) Thoppil RJ, Bishayee A, World J Hepatol. 2011, 3, 228–249.
- [3]. Walsh CT, Tang Y, Natural Product Biosynthesis (1st Ed.), The Royal Society of Chemistry, 2017.

- [4]. Yamada Y, Kuzuyama T, Komatsu M, Shin-Ya K, Omura S, Cane DE, Ikeda H, Proc. Natl. Acad. Sci. U. S. A 2015, 112, 857–862. [PubMed: 25535391]
- [5]. a)Gerber NN, Biotechnol. Bioeng 1967, 9, 321–327;b)Medsker LL, Jenkins D, Thomas JF, Koch C, Environ. Sci. Technol 1969, 3, 476–477.
- [6]. a)Citron CA, Gleitzmann J, Laurenzano G, Pukall R, Dickschat JS, Chembiochem 2012, 13, 202–214; [PubMed: 22213220] b)Hanson JR, Nat. Prod. Rep 2017, 34, 1233–1243; [PubMed: 28875214] c)Yamada Y, Cane DE, Ikeda H, in Meth. Enzymol, Vol. 515 (Ed.: Hopwood DA), Academic Press, 2012, pp. 123–162.
- [7]. a)Helfrich EJM, Lin G-M, Voigt CA, Clardy J, Beilstein J Org. Chem 2019, 15, 2889–2906;b)Yamada Y, Arima S, Nagamitsu T, Johmoto K, Uekusa H, Eguchi T, Shin-ya K, Cane DE, Ikeda H, J. Antibiot. (Tokyo) 2015, 68, 385–394. [PubMed: 25605043]
- [8]. Hoye TR, Jeffrey CS, Shao F, Nat. Protoc 2007, 2, 2451–2458. [PubMed: 17947986]
- [9]. Matsumori N, Kaneno D, Murata M, Nakamura H, Tachibana K, J. Org. Chem 1999, 64, 866–876. [PubMed: 11674159]
- [10]. Sauri J, Parella T, Magn. Reson. Chem 2013, 51, 509–516. [PubMed: 23780917]
- [11]. a)Cleves AE, Jain AN, Comput J. Aided Mol. Des 2017, 31, 419–439;b)Jain AN, Cleves AE, Gao Q, Wang X, Liu Y, Sherer EC, Reibarkh MY, Comput J. Aided Mol. Des 2019, 33, 531–558.
- [12]. Rinkel J, Rabe P, Chen X, Köllner TG, Chen F, Dickschat JS, Chem. – Eur. J 2017, 23, 10501–10505. [PubMed: 28696553]
- [13]. Li G, Dickschat JS, Guo YW, Nat. Prod. Rep 2020, 37, 1367–1383. [PubMed: 32458945]
- [14]. Biradi M, Hullatti K, Pharm. Biol 2017, 55, 1375–1379. [PubMed: 28317412]
- [15]. Chen B-W, Chao C-H, Su J-H, Tsai C-W, Wang W-H, Wen Z-H, Huang C-Y, Sung P-J, Wu Y-C, Sheu J-H, Org. Biomol. Chem 2011, 9, 834–844. [PubMed: 21109855]
- [16]. a)Sheu JH, Sung PJ, Su JH, Wang GH, Duh CY, Shen YC, Chiang MY, Chen IT, J. Nat. Prod 1999, 62, 1415–1420; [PubMed: 10543904] b)Sheu J-H, Sung P-J, Cheng M-C, Liu H-Y, Fang L-S, Duh C-Y, Chiang MY, J. Nat. Prod 1998, 61, 602–608; [PubMed: 9599257] c)Sung P-J, Su J-H, Wang G-H, Lin S-F, Duh C-Y, Sheu J-H, J. Nat. Prod 1999, 62, 457–463. [PubMed: 10096858]
- [17]. Pech-Puch D, Joseph-Nathan P, Burgueño-Tapia E, González-Salas C, Martínez-Matamoros D, Pereira DM, Pereira RB, Jiménez C, Rodríguez J, Sci. Rep 2021, 11, 496. [PubMed: 33436731]
- [18]. Blin K, Shaw S, Steinke K, Villebro R, Ziemert N, Lee SY, Medema MH, Weber T, Nucleic Acids Res. 2019, 47, W81–W87. [PubMed: 31032519]
- [19]. Johnson M, Zaretskaya I, Raytselis Y, Merezhuk Y, McGinnis S, Madden TL, Nucleic Acids Res. 2008, 36, W5–W9. [PubMed: 18440982]
- [20]. Zallot R, Oberg N, Gerlt JA, Biochemistry 2019, 58, 4169–4182. [PubMed: 31553576]
- [21]. a)Christianson DW, Chem. Rev 2017, 117, 11570–11648; [PubMed: 28841019] b)Driller R, Janke S, Fuchs M, Warner E, Mhashal AR, Major DT, Christmann M, Brück T, Loll B, Nat. Commun 2018, 9, 3971; [PubMed: 30266969] c)Driller R, Garbe D, Mehlmer N, Fuchs M, Raz K, Major DT, Bruck T, Loll B, Beilstein J Org. Chem 2019, 15, 2355–2368.
- [22]. a)Cyr A, Wilderman PR, Determan M, Peters RJ, J. Am. Chem. Soc 2007, 129, 6684–6685; [PubMed: 17480080] b)Rudolf JD, Dong L-B, Manoogian K, Shen B, J. Am. Chem. Soc 2016, 138, 16711–16721. [PubMed: 27966343]
- [23]. Peralta-Yahya PP, Ouellet M, Chan R, Mukhopadhyay A, Keasling JD, Lee TS, Nat. Commun 2011, 2, 483. [PubMed: 21952217]
- [24]. Li G, Guo Y-W, Dickschat JS, Angew. Chem. Int. Ed 2021, 60, 1488–1492.
- [25]. a)Nett RS, Montanares M, Marcassa A, Lu X, Nagel R, Charles TC, Hedden P, Rojas MC, Peters RJ, Nat. Chem. Biol 2017, 13, 69–74; [PubMed: 27842068] b)Zhang Q, Li H, Li S, Zhu Y, Zhang G, Zhang H, Zhang W, Shi R, Zhang C, Org. Lett 2012, 14, 6142–6145. [PubMed: 23205935]
- [26]. Rudolf JD, Chang C-Y, Ma M, Shen B, Nat. Prod. Rep 2017, 34, 1141–1172. [PubMed: 28758170]
- [27]. Gilchrist CLM, Chooi Y-H, Bioinformatics 2021, DOI 10.1093/bioinformatics/btab007.

- [28]. a)Kmail A, Lyoussi B, Zaid H, Saad B, Pharmacogn. Commun 2015, 5, 165–172;b)Mosmann T, J. Immunol. Meth 1983, 65, 55–63.
- [29]. a)CLSI, Methods for Dilution Antimicrobial Susceptibility Tests for Bacteria That Grow Aerobically. 11th Ed., Clinical and Laboratory Standards Institute: 950 West Valley Road, Suite 2500, Wayne, Pennsylvania 19087 USA, 2018;b)CLSI, Performance Standards for Antimicrobial Susceptibility Testing M100. 30th Ed., Clinical and Laboratory Standards Institute: 950 West Valley Road, Suite 2500, Wayne, Pennsylvania 19087 USA, 2020;c)Wiegand I, Hilpert K, Hancock RE, Nat. Protoc 2008, 3, 163–175. [PubMed: 18274517]

Author Manuscript

Author Manuscript

Author Manuscript

Author Manuscript

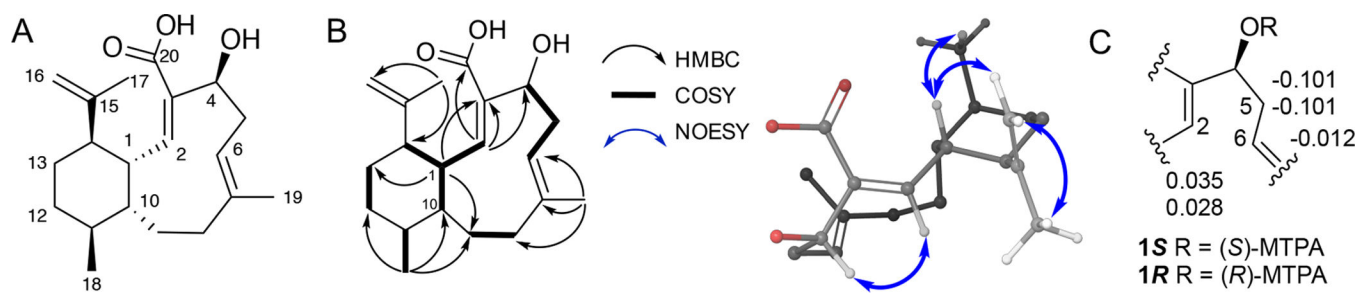


Figure 1.
 (A) Structure of benditerpenoic acid (**1**). (B) Key COSY, HMBC, NOESY correlations.
 (C) Modified Mosher's analysis of C-4 hydroxyl. Values given at C-2, C-5, and C-6 are $\delta_{(S)-(R)}$.

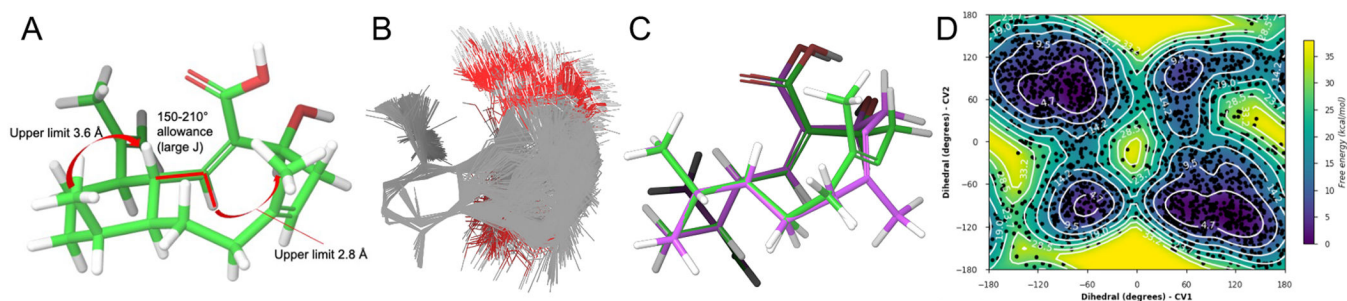


Figure 2.

(A) Three NMR-derived ForceGen restraints were utilized to generate an experimentally guided conformational search for **1**. (B) 693 conformations were found which exhibited no restraint violations. (C) DFT analysis of the conformer ensemble above produced a Boltzmann distribution in which the two lowest energy conformers (G 0.06 kcal mol⁻¹) exhibit a flip of the bicycle from 'methyl up' (green) to 'methyl down' (purple). (D) Metadynamics simulations indicate the barrier to flip is approximately 16 kcal mol⁻¹.

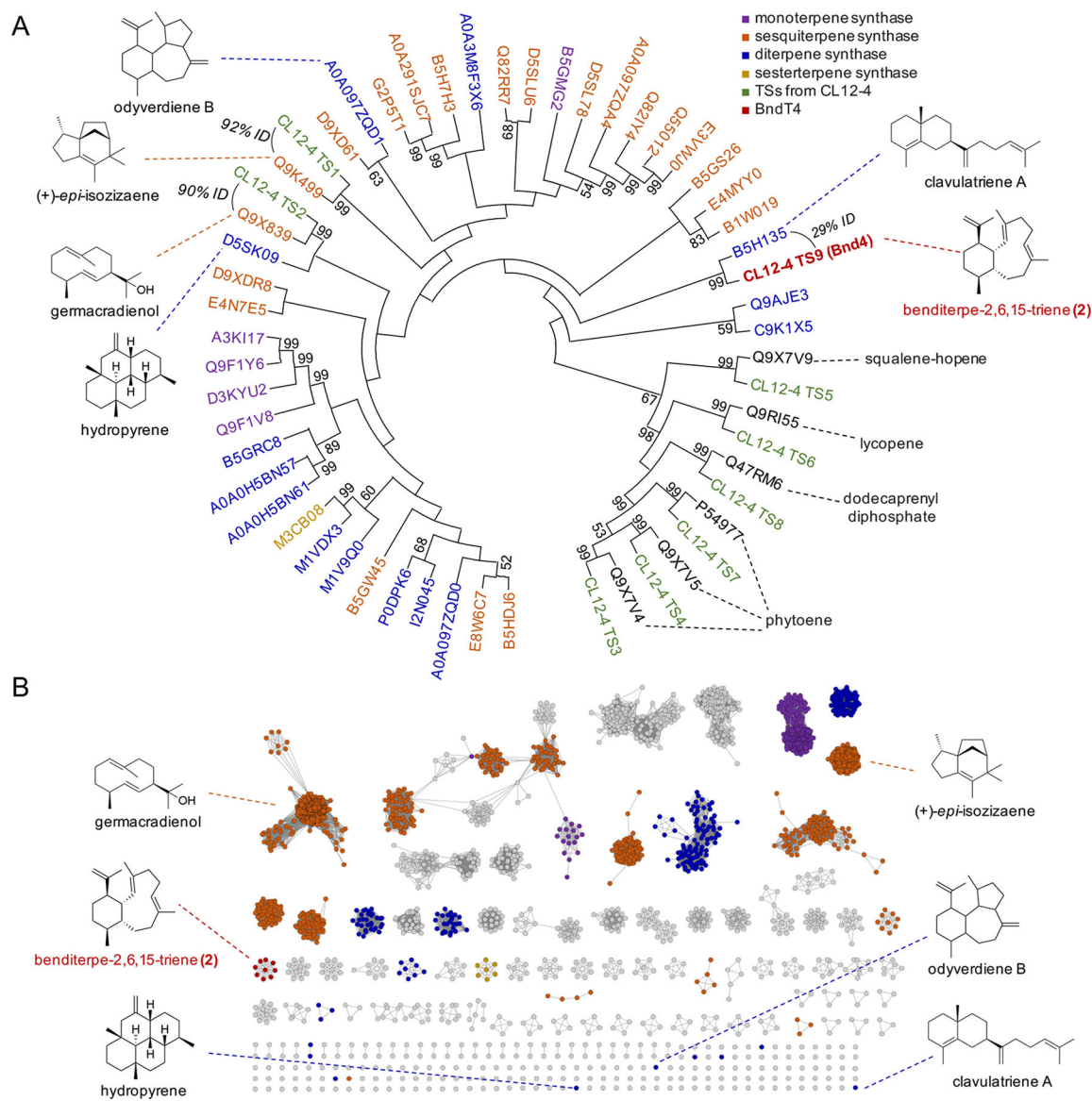


Figure 3.

Sequence analysis of the TSs found in *Streptomyces* sp. (CL12-4). (A) Phylogenetic analysis of the nine TSs found in the genome of CL12-4. Characterized TSs from *Streptomyces* are labeled with their UniProt accession numbers. Colored labels (shown in legend) indicate the type of terpene synthase. Structures discussed in the text are shown with their associated TSs. Bootstrap values >50% (based on 1000 resampled trials) are given at nodes. (B) Sequence similarity network of TSs from Streptomyceae at an e-value threshold of 10^{-60} . Clusters of TSs are colored corresponding to the legend in (A) and based on the characterized TSs found within. The eight homologous TSs from actinobacteria were included to highlight their similarity to Bnd4.

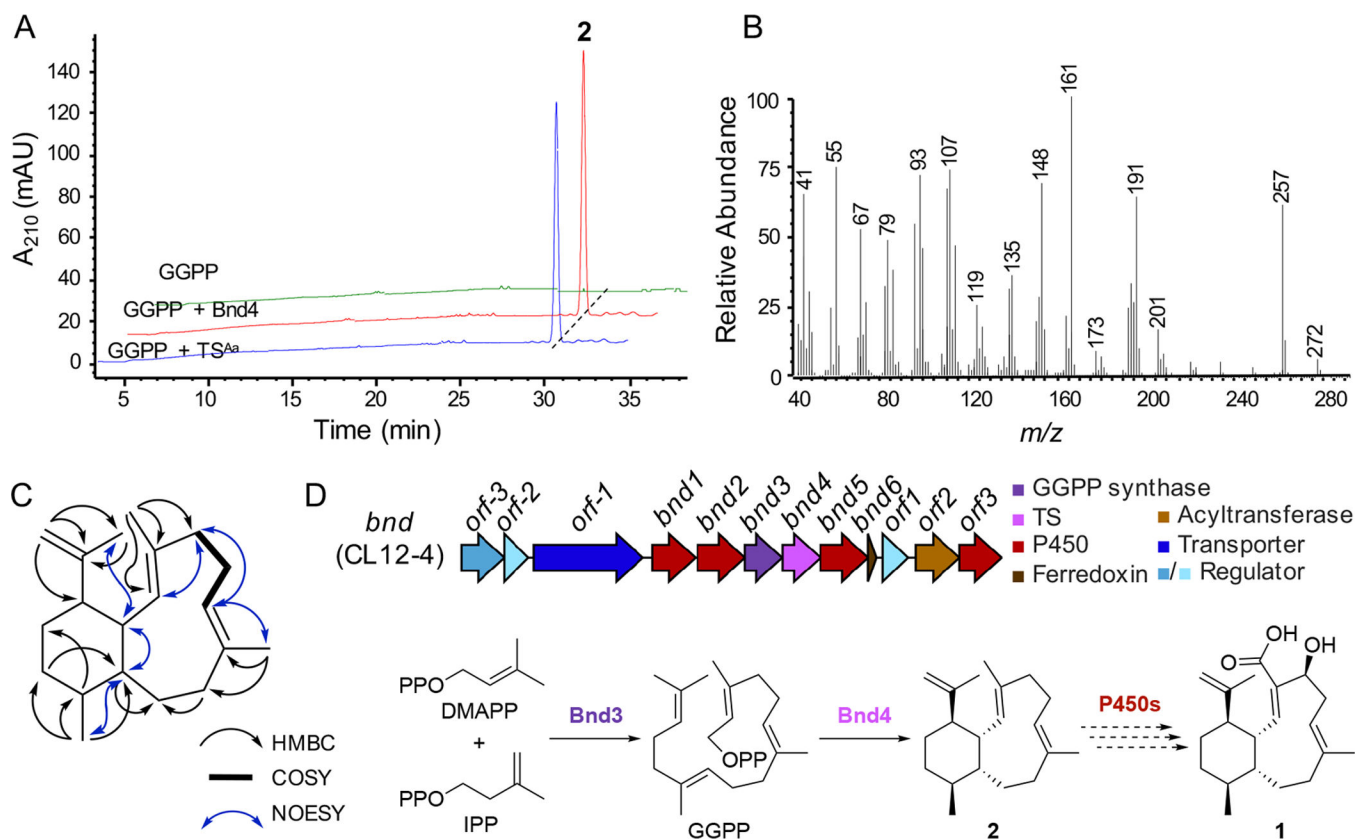


Figure 4. Biochemical characterization of Bnd4, structural elucidation of **2**, and biosynthesis of **1**. (A) Bnd4 and TS^{Aa} catalyze the cyclization of GGPP into **2**. Enzyme reactions, including a no enzyme control (GGPP), were analyzed by HPLC by monitoring at 210 nm. (B) GCMS spectrum of pure **2**. (C) Structure of **2** and key 2D NMR correlations supporting its structural assignment. (D) Biosynthetic gene cluster (*bnd*) and proposed biosynthetic pathway for **2**. The formation of **2**, a novel 6,10-bicyclic scaffold, by a unique TS, precedes oxidative tailoring affording **1**.

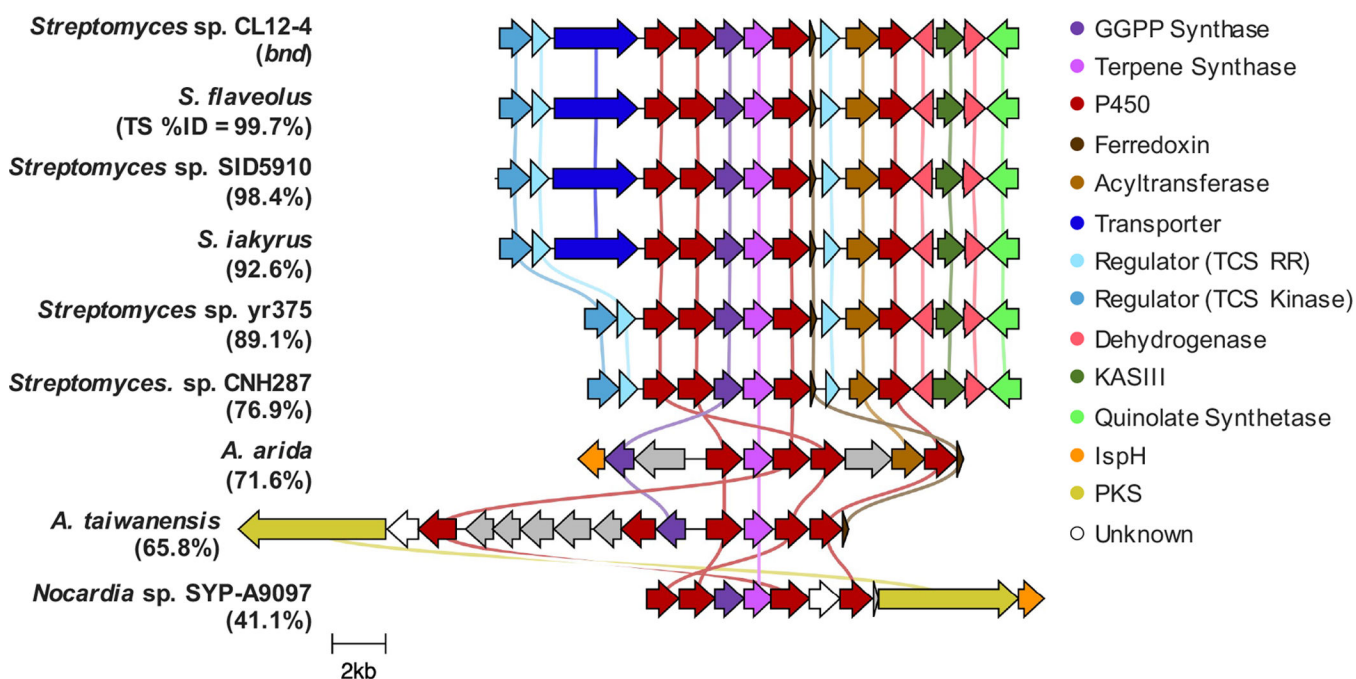


Figure 5. Comparative analysis of the *bnd* biosynthetic gene clusters. Genes are color-coded based upon their annotated Pfam or InterPro designations. The BGCs from the various *Streptomyces* spp. are almost all identical and are predicted to biosynthesize **1**. The BGCs from the two *Amycolatopsis* spp. and *Nocardia* sp. SYP-A9097 encode the core genes but possess different genes and genetic organization suggesting they produce the 6,10-bicyclic eunicellane-like core but biosynthesize different natural products.

Table 1.

Single dose testing of **1** and **2** against selected microorganisms (100 μM), given in percent cell survival, antibiotic controls were tested at 100 $\mu\text{g mL}^{-1}$. MIC assessment for **1** against Gram-positive pathogens ($\mu\text{g mL}^{-1}$).

	<i>E. faecium</i>	<i>S. aureus</i>	methicillin resistant <i>S. aureus</i>	multidrug resistant <i>S. aureus</i>	<i>B. subtilis</i>	<i>E. coli</i>	<i>P. aeruginosa</i>	<i>C. albicans</i>
Benditerpenoic acid (1)	102.1 \pm 1.1	49.7 \pm 3.6	59.5 \pm 2.5	50.2 \pm 3.5	1.1 \pm 0.9	125.4 \pm 1.9	95.3 \pm 0.4	125.0 \pm 6.9
Benditerpe-2,6,15-triene (2)	112.5 \pm 1.1	86.9 \pm 6.0	95.2 \pm 1.0	103.3 \pm 1.4	48.4 \pm 12.3	133.1 \pm 3.5	97.7 \pm 0.7	224.6 \pm 3.0
Kanamycin	-	0.0 \pm 0.5	0.0 \pm 0.0	-	-	-	-	-
Vancomycin	0.0 \pm 0.0	-	0.4 \pm 0.4	0.0 \pm 0.0	0.6 \pm 0.3	0.0 \pm 0.3	0.3 \pm 0.7	-
Chloramphenicol	-	-	-	-	0.0 \pm 0.0	11.9 \pm 4.2	0.0 \pm 0.1	-
Amphotericin B	-	-	-	-	-	-	-	0.0 \pm 13.7
Benditerpenoic acid (1) MIC	128	64	64	128	32	-	-	-